

Available online at [www.sciencedirect.com](http://www.sciencedirect.com)

SCIENCE @ DIRECT®

Surface &amp; Coatings Technology 200 (2005) 1683–1689

[www.elsevier.com/locate/surfcoat](http://www.elsevier.com/locate/surfcoat)

# Thermal stability and microstructure characterization of CrN/WN multilayer coatings fabricated by ion-beam assisted deposition

Yan-Zuo Tsai, Jenq-Gong Duh\*

*Department of Materials Science and Engineering, National Tsing Hua University, Hsinchu, Taiwan*

Available online 13 September 2005

## Abstract

CrN/WN multilayer coatings were deposited on both silicon (100) and stainless steel substrate by the ion-beam assisted deposition. The bilayer periods were designed and controlled in the range from 3 nm to 30 nm. The CrN/WN films were annealed from 750 °C to 850 °C for 1 and 4 h in vacuum to evaluate the thermal stability of these coatings. The difference of microstructural characterization between the CrN/WN multilayer coating and the CrN single layer coating was investigated by scanning electron microscopy. The phase transformation after annealing was probed by X-ray diffraction. The hardness of as-deposited CrN/WN coating with 8 nm bilayer period was much higher than that of CrN and WN single layers. The thermal stability of CrN/WN multilayer coatings with different bilayer periods was also discussed in correlation to the associated microstructural evolution.

© 2005 Elsevier B.V. All rights reserved.

**Keywords:** CrN; CrN/WN; IBAD; Superlattice; Nanolayer; Hardness

## 1. Introduction

Due to the excellent performance in hardness, wear and corrosion resistance, the transition metal nitrides have been taken for hard protective coating [1,2]. In the nitride systems, the chromium nitride (CrN) films have been investigated for years, and proved to exhibit good mechanical performance, thermal properties and anti-oxidation behaviours [3,4]. Recent studies also show that multilayer coatings composed of two kinds of transition nitride films exhibit superior mechanical strength, such as hardness, adhesion, and wear resistance, as compared to single layer nitride coating due to their specific interfaces [5–7]. Several new material systems, including TiN/AlN, TiN/NbN, CrN/TiN and CrN/AlN, exhibit evident enhancement of micro-hardness [7–10]. Theoretically, the enhanced hardness could be explained by dislocation blocking between interfaces, due to the shear moduli difference, and by coherency strain from lattice mismatch of the two different

material systems [11]. The multilayer coatings sustain high hardness at the room temperature, however, after heat treatment at elevated temperature in vacuum, the strength of multilayer coatings would be degraded rapidly, which was caused by the vanishing of nanolayered structure due to the inter-diffusion of atoms. The thermal stability is thus a critical issue and plays an important role on performance of tools operated at the elevated temperature in vacuum. In this study, the combination of chromium nitride and tungsten nitride coating was proposed to form a nanostructure coating system. Efforts were concentrated on the structural characterization and thermal stability of both CrN and CrN/WN coatings with bilayer periods of 3 nm to 30 nm in vacuum environment. The microstructure of CrN and CrN/WN multilayer coatings were analyzed by X-ray diffraction and SEM. In addition, the strength of the deposit under various conditions was investigated by nanoindentation.

## 2. Experimental details

The CrN single layer coating and CrN/WN multilayer coatings were fabricated on the silicon (100) and AISI

\* Corresponding author. Fax: +886 3 5712686.

E-mail address: [jgd@mx.nthu.edu.tw](mailto:jgd@mx.nthu.edu.tw) (J.-G. Duh).

Table 1

Layer configuration and microhardness of the CrN/WN multilayer coatings

Sample name	Bilayer period (nominal) (nm)	Bilayer period (calculated) (nm)	$\Delta 2\theta$ (deg)	Microhardness (GPa)
041126	30	29.4	0.30	25.0
041028	10	11.4	0.77	24.5
041105	8	8.4	1.05	29.1
041116	5	5.6	1.57	24.5
041207	3	3.2	2.76	25.6

420 tool steel substrate by ion-beam assisted deposition (IBAD). Metallurgical finishing and polishing with SiC sandpapers of #120, #240, #400, #600, #800, and #1200 were used to remove the contamination on the surface of steel substrate. To obtain an adequate surface condition for the following tests and property evaluation, the ground substrates were then polished with a 1.0  $\mu\text{m}$  diamond powder. After grinding and polishing treatment, the substrates were cleaned by ultrasonic vibration cleaning in acetone to remove all contaminants. Both chromium and tungsten target of 3 in. in diameter were 99.99 wt.% in purity. After loading of the substrates and targets, the vacuum chamber was degassed down to  $2.1 \times 10^{-4}$  Pa, followed by the inlet of argon and nitrogen gases as plasma source and reactive gas, respectively, to a working pressure of  $1.2 \times 10^{-1}$  Pa. The target-to-substrate distance was fixed at 100 mm from sputtering target sources and ion gun. Before deposition, both chromium and tungsten targets were pre-sputtered for 2 min to clean the target surface, and then Cr interlayer was deposited with a power of 300 W for 2 min. An assisted ion source (Mark II Gridless ion source, Veeco) was adopted during sputtering.

The current of assisted ion beam and electron beam were 4.0 and 2.7 A, respectively. Sputtering of Cr and W was proceeded alternately to form the sequential CrN/WN multilayer coating. Both the input power on Cr and W target were fixed at 300 W. The deposition time of individual nitride layer of the multilayer CrN/WN coating during sequential sputtering was modified from 8 to 93 s. The total thickness of every multilayer coating with different bilayer periods was controlled around 1.0  $\mu\text{m}$ . The CrN/WN multilayer coatings were then annealed at 750, 800 and 850  $^{\circ}\text{C}$  in a vacuum chamber with a pressure of  $6.7 \times 10^{-4}$  Pa for 1 h and 4 h.

The multilayer structure and crystallographic phases of the thin film were identified by low-angle and high angle diffraction, respectively, with an X-ray diffractometer (Shimadzu, XRD6000) under  $\theta/2\theta$  mode. The coating thickness and cross-section image were observed with a field emission scanning electron microscope (FESEM, JSM-6500, JEOL, Japan). The microhardness of the coatings was analyzed with a nanoindentation apparatus (TriboScope, Hysitron, Minneapolis, MN) equipped with a Berkovich indenter. The maximum load adopted for all the coating was fixed at 3000  $\mu\text{N}$ .

### 3. Results and discussion

#### 3.1. Low-angle X-ray diffraction

The CrN/WN multilayer coatings were fabricated with total thickness about 1.0  $\mu\text{m}$  by IBAD process. By controlling the deposition time of individual nitride layer,

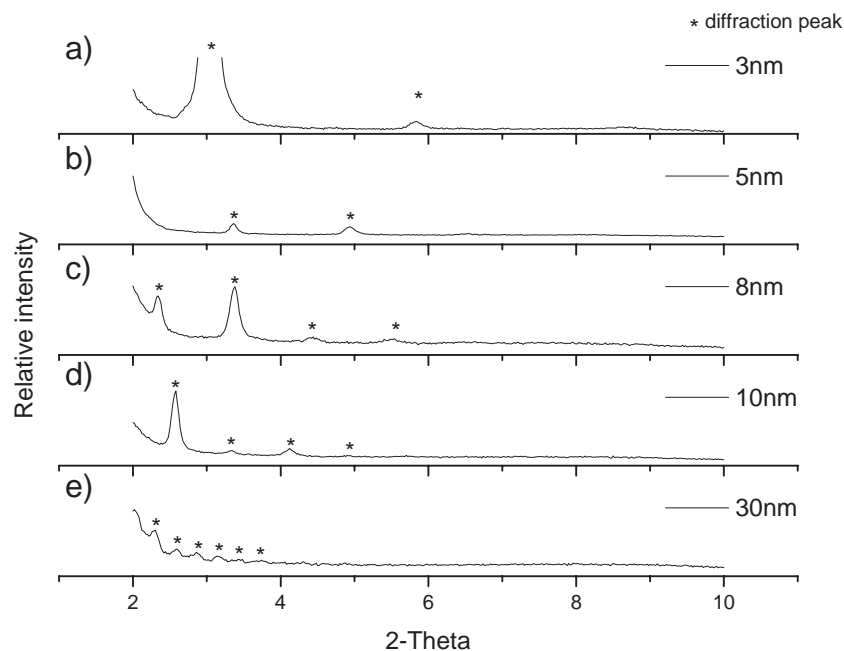


Fig. 1. Low-angle X-ray diffraction spectra of CrN/WN multilayer coatings with adjusted bilayer period (a)  $A=3$ , (b)  $A=5$ , (c)  $A=8$ , (d)  $A=10$  and (e)  $A=30$  nm.

the bilayer period was adjusted. The nominal bilayer periods are listed in Table 1. The low-angle X-ray diffraction spectra of CrN/WN multilayer coatings with adjusted bilayer period  $\Lambda=3, 5, 8, 10$  and  $30$  nm is presented in Fig. 1. It was demonstrated by Li et al. [12] that modulation interfaces of multilayer coatings with compositionally modulated structure can produce diffraction of X-ray. Because the interplanar distance of crystals are usually smaller than bilayer periods of multilayer coatings, only at low angle can the diffraction peaks resulting from modulation interfaces be observed. There are two evident diffraction peaks found in

the low-angle XRD pattern for  $\Lambda=3$  nm, and four peaks for  $\Lambda=8$  nm, and six peaks for  $\Lambda=30$  nm. With increasing bilayer period, the amount of diffraction peak increased, while the space between two peaks decreased in every low-angle XRD pattern. According to the low-angle XRD peaks, it is apparent that CrN/WN multilayer coatings prepared by IBAD possess a dense and well-packed layered coating configuration. Thus, smooth and clear interfaces between CrN and WN layers are evident.

Fig. 2a and b show the low-angle X-ray diffraction spectra of CrN/WN multilayer coatings with bilayer period

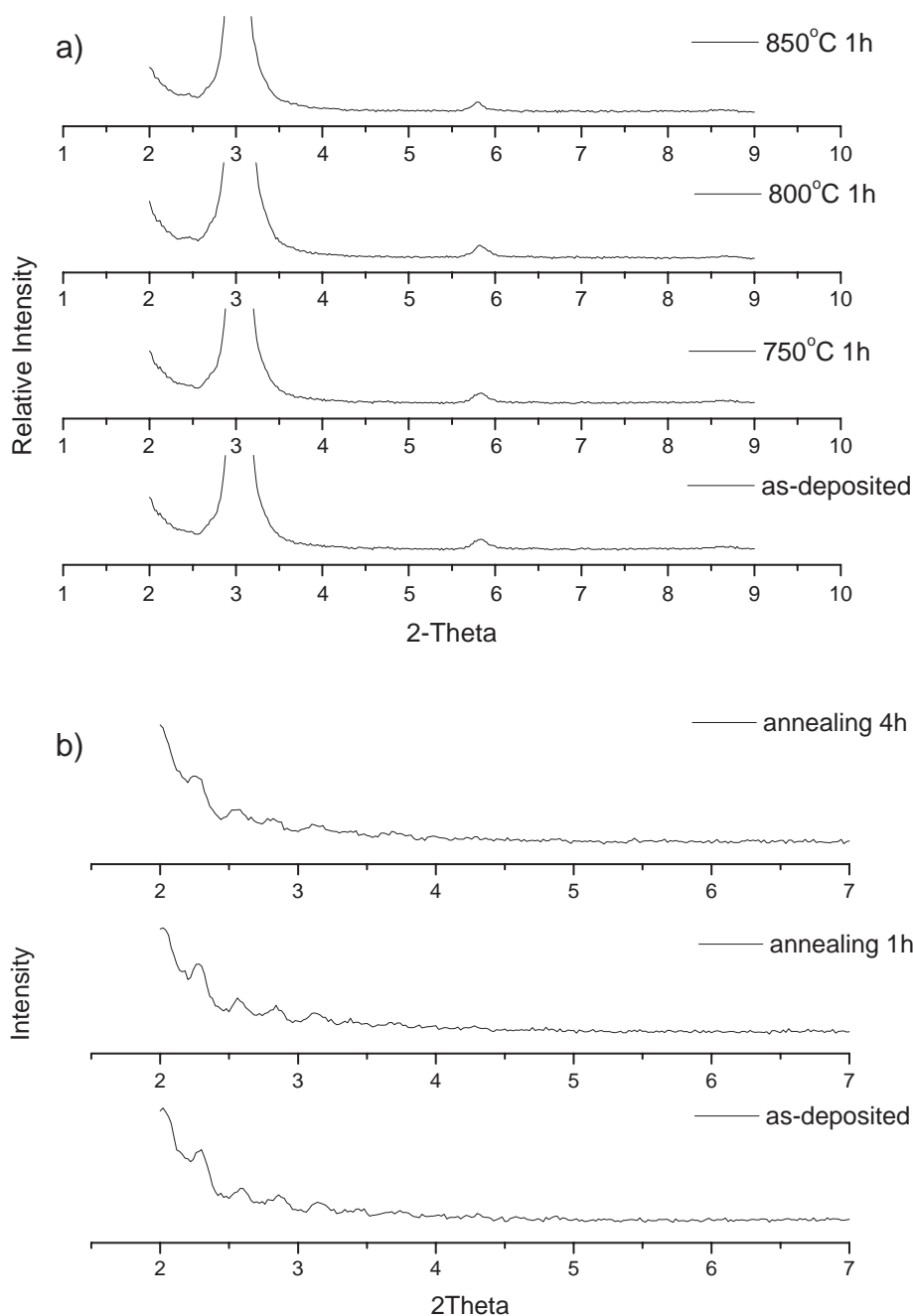


Fig. 2. Low-angle X-ray diffraction spectra of CrN/WN multilayer coatings (a) with bilayer period of 3 nm after annealing at various temperatures and (b) with bilayer period of 30 nm after annealing for different time.

of 3 nm after annealing at different temperature and that with bilayer period of 30 nm after annealing for different time, respectively. In Fig. 2a, the low-angle XRD peaks do not vanish after heat treatment at 850 °C for 1 h, and nothing more than the second peak of this spectra is weakened slightly. Due to the existence of the low-angle diffraction peaks, the individual layer of chromium nitride and tungsten nitride should be unmixed after annealing. No interdiffusion between CrN and WN interfaces in the coating with bilayer period of 3 nm was revealed after thermal treatment, so the thermal stability of the film was evidenced. The low-angle XRD peaks of coating with bilayer period of 30 nm after 800 °C annealing for 4 h shown in Fig. 2b are weaker and broader than that of as-deposited film. The sharpness of interlayer was decreased due to the interdiffusion after heat treatment. Nevertheless, the superlattice structure still existed.

The bilayer period of multilayer films can be enumerated from Bragg's Law [12]:

$$\sin^2\theta = \left(\frac{n\lambda}{2A}\right)^2 + 2\delta \quad (1)$$

where  $A$  is the bilayer period,  $\lambda$  is the wavelength of Cu  $K\alpha=0.154$  nm,  $\delta$  is the real part of the average refractive index of the coating and  $\theta$  is the interval of two peaks of the low-angle XRD pattern. Both the enumerated bilayer periods and  $\theta$  are listed in Table 1. The difference between

nominal and enumerated bilayer periods is no more than 10%. Since the scale of modulation periods is small in the nanoscale, it is apparent that the measured values of bilayer thickness in this work were very close to the expected one. Table 1 also lists the microhardness of CrN/WN multilayer films with different modulation period. The hardness of multilayer coating with modulation period of 8 nm is about 29 GPa. It is argued that when the multilayer formed a superlattice structure, the hardness of this coating would increase.

### 3.2. High angle X-ray diffraction

The high angle X-ray diffraction patterns of superlattice films with modulation period of 8 nm at as-deposited state and 800 °C annealing for 1 h in vacuum are shown in Fig. 3. Four broadened diffraction peaks are found approximately at  $2\theta=37^\circ$ ,  $43^\circ$ ,  $62^\circ$  and  $74^\circ$  in the as-deposited film, so the face centered cubic phase of CrN/WN multilayer is evidenced. Although it was difficult to identify chromium and tungsten nitrides due to overlapped diffraction peaks (CrN (111):  $37.5^\circ$ , WN (111):  $37.7^\circ$  [18]) by XRD patterns, the satellite peaks near the peak (111) of the f.c.c. structure were found, which confirmed the formation of superlattice structure [13]. Because of the broadening and the weak intensity for the peaks, the grain size of the film was supposed to be small.

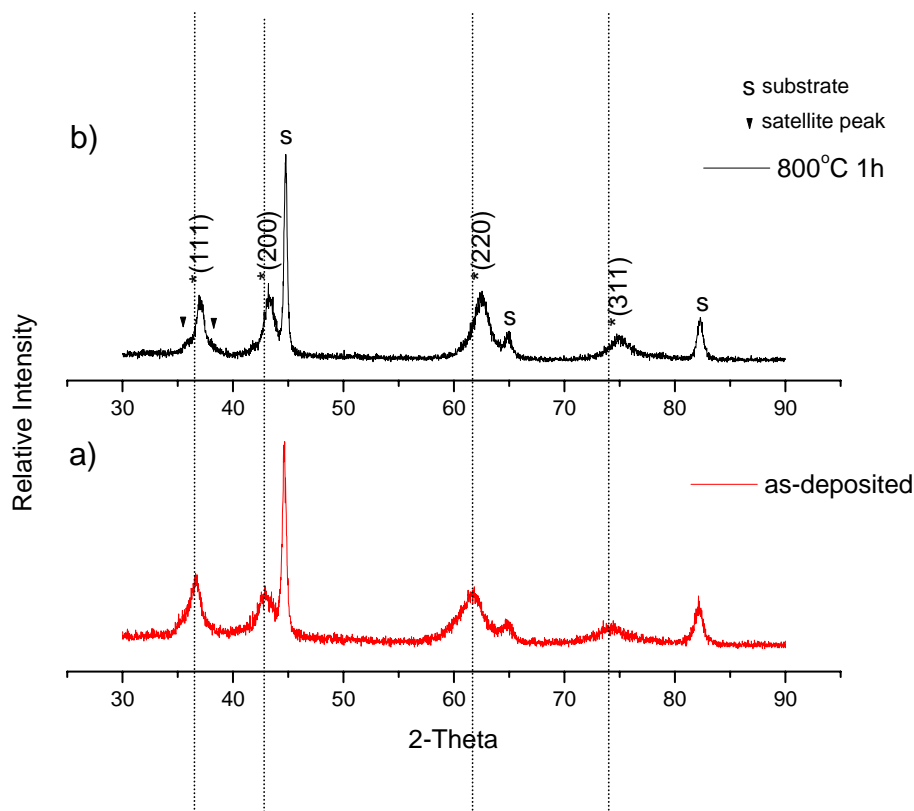


Fig. 3. High angle X-ray diffraction patterns of superlattice films with modulation period of 8 nm (a) as-deposited state, and (b) 800 °C annealing for 1 h in vacuum.

It was also found that the satellite peaks still existed and intensity of every Bragg diffraction peak increased after annealing at 800 °C for 1 h in vacuum. It was argued that the superlattice structure prevailed and the grain growth occurred after heat treatment. Because an in-plane compressive stress usually existed in crystalline coatings deposited by sputtering [14], all the four Bragg diffraction peaks were smaller than the f.c.c. diffraction peaks of CrN (or WN) by 1° or 2°. After heat treatment, the four main peaks shifted to higher angle apparently, because the compressive stress was released. In fact, the main diffraction peak positions of this film after thermal treatment shifted toward that of CrN(or WN).

Similar observation could be revealed in the multilayer film with modulation period of 3 nm. Fig. 4 shows the high angle X-ray diffraction patterns of multilayer films with bilayer period of 3 nm at as-deposited state and 800 °C annealing for 1 and 4 h in vacuum. The four Bragg diffraction peaks of CrN/WN superlattice existed and satellite peaks could also be found. By heat treatment, the compressive stress was released so the four diffraction peaks shifted to higher angle obviously. With increasing thermal treatment time, more compressive stress was released and thus the peak was shifted more toward higher angle. The positions of the four main peaks then moved toward that of CrN (or WN).

It was proved that the multilayer film with bilayer period of 3 nm exhibited superlattice structure by the appearance of

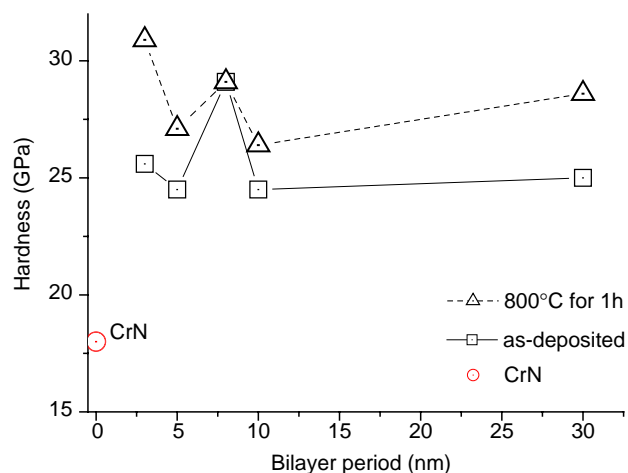


Fig. 5. The hardness vs. bilayer period of CrN/WN multilayer coatings.

the satellite peaks around (111) and (311) peaks of f.c.c. structure. The position of the satellite peaks is given by [15]:

$$\sin\theta_{\pm} = \sin\theta_B \pm m\lambda/2\Lambda \quad (2)$$

where  $\theta_B$  is the position of main peak,  $\lambda$  is the wave length of Cu  $K\alpha=0.154$  nm,  $\Lambda$  is the modulation period and  $\theta_{\pm}$  is the position of satellite peaks. If the modulation period of multilayer coatings decreased, the space between the satellite peaks and the main Bragg diffraction peaks increased. Nevertheless, due to the broadened (311) peak

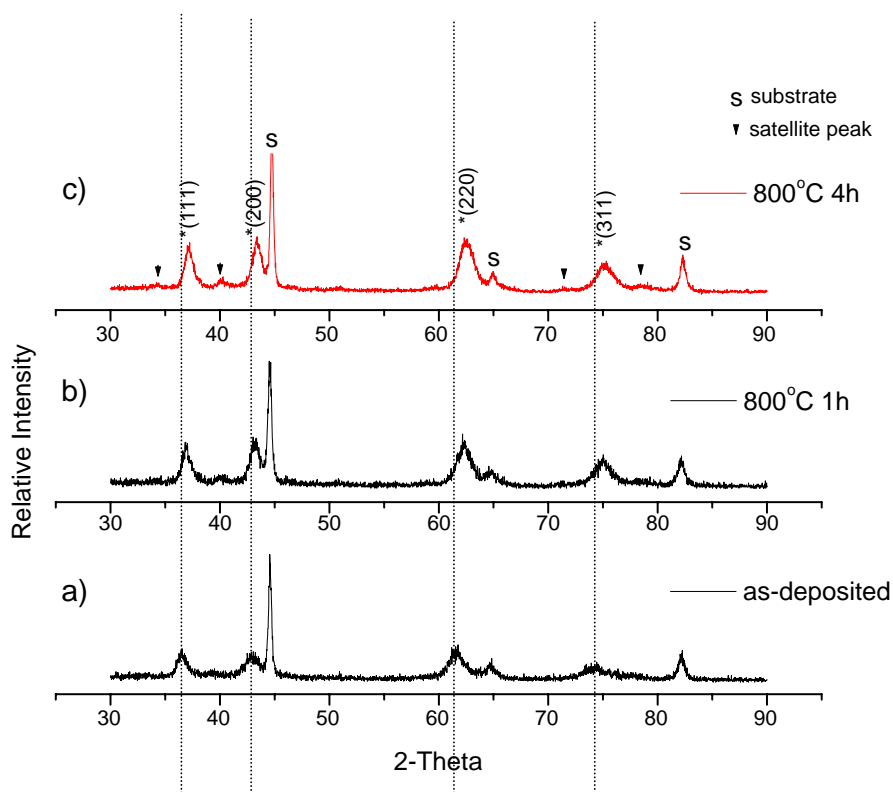


Fig. 4. High angle X-ray diffraction patterns of multilayer coatings with bilayer period of 3 nm (a) as-deposited state, (b) 800 °C annealing for 1 h in vacuum, and (c) 800 °C annealing for 4 h in vacuum.



of the coating with bilayer period of 8 nm, the satellite peaks were overlapped and could not be observed.

### 3.3. Microhardness and SEM images

The hardness of CrN/WN multilayer coatings as a function of modulation period as well as the microhardness of CrN is shown in Fig. 5. The hardness of CrN is about 18 GPa and those of all the multilayer coatings are over 24 GPa. The nanolayered structure of the multilayer films indeed promoted the hardness of the coatings. The microhardness of coating with modulation period of 8 nm is 29.1 GPa. The abruptly raised hardness have been reported [5,8,15,16] and the superlattice enhancement of mechanical properties was proposed. In theory, the enhanced hardness could be explained by dislocation blocking between interfaces due to the different shear moduli, and by coherency strain from lattice mismatch of the two different material systems [11].

It is interesting to point out that in this study the hardness seemed to increase after 800 °C annealing for 1 h, instead of falling-off. The superlattice structure was maintained after

annealing, indicating that the thermal stability of the multilayer film is quite superior. It is noted that the peak intensity increased after heat treatment, as shown in Fig. 4. This would be attributed to the increase of crystallinity, leading to the enhancement of microhardness, as indicated in Fig. 5.

The cross-section SEM images of CrN and CrN/WN multilayer coating with bilayer period of 8 nm are shown in Fig. 6a and b, respectively. Smooth and dense coating configurations were developed by IBA process. CrN deposit revealed strong columnar structure in Fig. 6a, and a tight and dense structure of CrN/WN multilayer coating is exhibited in Fig. 6b. The difference of hardness between CrN and CrN/WN multilayer coatings may be ascribed to the cross-sectional structural variation. The superior microhardness of multilayer coating with modulation period of 8 nm was due to the dense structure. However, owing to the resolution limit, the nanolayered structure of multilayer film could not be observed by SEM only. More attempts in the TEM analysis for the microstructure details of the multilayer film should be scheduled in the future work.

### 4. Conclusions

The CrN/WN multilayer coatings fabricated by ion-beam assisted deposition (IBAD) process exhibited a dense and well-packed layered structure, and the interfaces between CrN and WN layers were smooth and evident. This confirmation of the layered structure of CrN/WN coatings could be achieved by low-angle X-ray diffraction technique. It was believed that the CrN/WN multilayer films formed a superlattice structure by the appearance of satellite peaks from high angle X-ray diffraction patterns. By comparing the cross-section image of CrN coating and CrN/WN multilayer film, it was apparent that the superior microhardness showed up with the nanolayered structure. The microhardness was enhanced due to the existence of superlattice structure. The evidence of superlattice structure was also revealed by the hardness enhancement in the multilayer coating with modulation period of 8 nm. After heat treatment at various temperatures, all the specific characteristic peaks of low-angle and high angle X-ray diffraction patterns still prevailed without appreciable diminishing. The hardness enhancement of multilayer coatings still existed and seemed to be even higher after 800 °C annealing for 1 h. As a result, the thermal stability of the CrN/WN multilayer coatings was excellent as compared with other nitride multilayer films [17], and this material system could be employed for high temperature applications.

### Acknowledgment

This support of work from the National Science Council, Taiwan, under Contract No. NSC 93-2216-E-007-013 is appreciated.

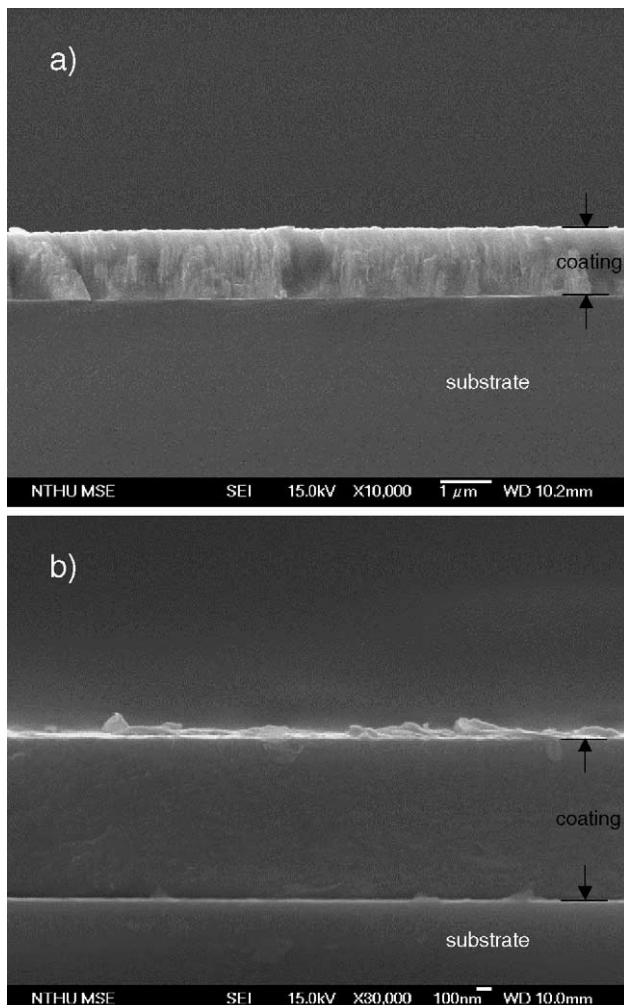


Fig. 6. Cross-sectional SEM image of (a) CrN coating and (b) CrN/WN multilayer coating with modulation period of 8 nm.

## References

- [1] P. Hones, R. Consiglio, N. Randall, F. Levv, *Surf. Coat. Technol.* 125 (2000) 179.
- [2] T. Hurkmans, T. Trinh, D.B. Lewis, J.S. Brooks, W.D. Munz, *Surf. Coat. Technol.* 76–77 (1995) 159.
- [3] J.A. Sue, T.P. Chang, *Surf. Coat. Technol.* 76–77 (1995) 61.
- [4] F.B. Wu, J.J. Lee, J.G. Duh, *Thin Solid Films* 377–378 (2000) 354.
- [5] M.S. Wong, G.Y. Hsiao, S.Y. Yang, *Surf. Coat. Technol.* 133–134 (2000) 160.
- [6] C. Ducros, V. Benevent, F. Sanchette, *Surf. Coat. Technol.* 163–164 (2003) 681.
- [7] M. Setoyama, M. Irie, H. Ohara, M. Tsujioka, Y. Takeda, T. Nomura, N. Kitagawa, *Thin Solid Films* 341 (1999) 126.
- [8] L. Hultman, C. Engstrom, M. Oden, *Surf. Coat. Technol.* 133–134 (2000) 227.
- [9] P. Yashar, S.A. Barnett, J. Rechner, W.D. Sproul, *J. Vac. Sci. Technol., A* 16 (1998) 2913.
- [10] G.S. Kim, S.Y. Lee, J.H. Hahn, S.Y. Lee, *Surf. Coat. Technol.* 171 (2003) 91.
- [11] X. Chu, S.A. Barnett, *J. Appl. Phys.* 77 (1995) 4403.
- [12] G.Y. Li, Z.H. Han, J.W. Tian, J.H. Xu, M.Y. Gu, *J. Vac. Sci. Technol., A* 20 (2002) 674.
- [13] H.C. Barshilia, A. Jain, K.S. Rajam, *Vacuum* 72 (2004) 241.
- [14] G. Abadias, Y.Y. Tse, A. Michael, C. Jaouen, M. Jaouen, *Thin Solid Films* 433 (2003) 166.
- [15] P.C. Yashar, W.D. Sproul, *Vacuum* 55 (1999) 179.
- [16] D.G. Kim, T.Y. Seong, Y.J. Baik, *Surf. Coat. Technol.* 153 (2002) 79.
- [17] Q. Yang, L.R. Zhao, *J. Vac. Sci. Technol., A* 21 (2003) 558.
- [18] JCPDS card: 65-2898.